Biodegradation **15:** 435–451, 2004.

Modeling natural attenuation of chlorinated ethenes under spatially varying redox conditions

Mark A. Widdowson
The Charles E. Via, Jr. Department of Civil and Environmental Engineering, Virginia Polytechnic Institute and State University, 220A Patton Hall, Blacksburg, VA 24061-0105, USA (e-mail: mwiddows@vt.edu)

Accepted 13 April 2004

Abstract

A three-dimensional model for the transport and reductive dechlorination of chlorinated ethenes in ground-water systems with variable redox conditions is demonstrated and applied to a pilot test for accelerated natural attenuation of trichloroethene (TCE). The rate and extent of biotransformation of TCE and chlorinated progeny is controlled by the dominant terminal electron accepting process (TEAP) that is simulated over space and time. The solute transport code, Sequential Electron Acceptor Model, 3D-transport, (SEAM3D) which simulates aerobic and sequential anaerobic biodegradation of organic carbon, is modified to implement the equations. Results of a generic model for TCE transport in ground-water systems with different redox conditions demonstrate that the degree of chlorinated ethene attenuation is influenced by background concentrations of aqueous- and solid-phase electron acceptors, but that model results are sensitive to other input parameters (inhibition coefficients, maximum rate of reductive dechlorination, biomass concentrations, and ground-water velocity). Simulation results of enhanced *in situ* bioremediation using dissolved organic carbon as a reducing agent show that spatial and temporal changes in the dominant TEAP and the subsequent rate of reductive dechlorination are adequately represented with the model. Initial concentrations of Fe(III) and the dechlorinating microbial population influence the simulated time lag observed during the pilot test.

Introduction

Chlorinated ethenes, particularly tetrachloroethene (PCE) and trichloroethene (TCE), are cited as the two of the most common contaminants in groundwater (Charbaneau 2000). Chlorinated ethene plumes are known to persist in groundwater systems where the natural attenuation capacity is insufficient to meet site-specific remediation objectives (Chapelle & Bradley 1998). However, under suitable conditions, monitored natural attenuation (MNA) can be an effective strategy for restoring aquifer systems contaminated with chlorinated solvents, particularly in combination with an engineered remedial action (ERA) that promotes *in situ* remediation or containment (EPA 1999; NRC 2000). At many sites where MNA is implemented, biological processes are an important component of the natural attenuation of chlorinated ethenes (Wiedemeier et al. 1998).

Chlorinated ethenes are subject to a range of microbial degradation processes that include reductive dechlorination (Vogel & McCarty 1985), aerobic oxidation (Hartmans et al. 1985, and others), anaerobic oxidation (Bradley & Chapelle 1996, and others), and aerobic cometabolism (Wilson & Wilson 1985, and others). The most critical attenuation process, reductive dechlorination, in which PCE and/or TCE and chlorinated daughter products – *cis*-1,2-dichloroethene (*cis*DCE), and vinyl chloride (VC) – are reduced to ethene and ethane, has been observed in numerous anaerobic chloroethene-contami-

nated aquifers, but the extent of dechlorination is highly variable from site to site (Chapelle 2001).

Reductive dechlorination of chloroethene contaminants will be sustained as long as reducing conditions and an ample supply of electron donor are maintained and dehalogenating organisms are present (Bradley 2000). Organic carbon, which is fermented to produce hydrogen, is either supplied naturally or is derived from contaminant sources (e.g., petroleum hydrocarbons) that co-mingle with a chlorinated ethane plume (Wiedemeier et al. 1998). If the redox condition of a ground-water system does not favor reductive dechlorination, reducing agents – hydrogen release compounds (HRC; Koenigsberg et al. 2000), vegetable oil (Boulicault et al. 2000), dissolved organic compounds (Casey et al. 2002), and molasses (Hansen et al. 2000) – may be supplied to the aquifer to increase the rate of reductive dechlorination. ERAs designed to promote reductive dechlorination rely on either passive mixing, in which reducing agents are transported by the natural hydraulic gradient, or active mixing by forced gradients (e.g., injection–recovery systems). In these situations, quantitative tools are needed to assess the impact of organic carbon addition on the reductive dechlorination (i.e., accelerated natural attenuation) and evaluate the effect and sustainability of a reducing agent in the aquifer over the time.

To address this deficiency, Widdowson (2003) recently revised the Sequential Electron Acceptor Model for 3D transport, (SEAM3D) code to incorporate the fate and transport of chlorinated ethenes coupled to the simulated terminal electron-accepting processes (TEAPs). Waddill & Widdowson (1998, 2000) developed SEAM3D to simulate organic carbon sources and temporal and spatial variability of redox conditions in a ground-water system. The purpose of this paper is to present (1) model applications of reductive dechlorination under variable redox conditions and (2) field testing of SEAM3D at a TCE-contaminated site where a dissolved organic substrate was delivered to promote *in situ* bioremediation. The paper presents a summary of the mathematical model, model applications for passive and active *in situ* bioremediation, and simulation results of the field test.

Model overview

Conceptual model

SEAM3D is comprised of modules for physical transport and sorption build upon the code MT3DMS (Zheng & Wang 1999) and four additional modules: biodegradation, reductive dechlorination, cometabolism, and NAPL Dissolution Packages (Widdowson 2003). SEAM3D can simulate the 3D transport of PCE or TCE (as the parent compound) and daughter products of reductive dehalogenation coupled to relevant biological processes in aquifers: direct oxidation, reductive dehalogenation, and cometabolism. The SEAM3D Biodegradation Package simulates the direct oxidation of organic carbon substrate for the complete range of TEAPs – aerobic and sequential anaerobic (nitrate-, Mn(IV)-, Fe(III)-, sulfate-reduction and methanogenesis) subject to electron acceptor (EA) availability (Waddill & Widdowson 1998). In SEAM3D, the TEAP distribution is solved simultaneously with the chlorinated ethane transport equations so that the rate of each applicable biotransformation process depends on the model-simulated redox condition in each model cell of the finite-difference grid (Waddill & Widdowson 2000; Widdowson 2003).

Each chlorinated ethene (PCE, TCE, *cis* DCE, and VC) may serve as an EA when subject to reductive dechlorination in the absence of oxygen or nitrate (Widdowson 2003). These compounds are known to be reduced under anaerobic conditions in which dissolved hydrogen (not explicated modeled) is the assumed electron donor (Chapelle 2001). Reductive dechlorination will proceed at a maximum rate under methanogenesis and will be inhibited to some extent in model cells where higher-energy yielding TEAPs are dominant, beginning with sulfate reduction. Among the four chlorinated ethenes, the yield of energy decreases with the number of chlorine atoms so that the parent compound (in this study, TCE) will be preferentially used over daughter products (*cis*DCE and VC).

Governing equations

Expressions for mass balance of aqueous phase constituent transport are described for each biodegradable substrate, EA, biodegradation end

product, and chlorinated ethene. These equations incorporate advective–dispersive transport, microbially-mediated biotransformation, sorption and dissolution from the NAPL phase. For the growth substrate introduced to promote reductive dechlorination, the equation of mass balance is

$$-\frac{\partial}{\partial x_i}(v_i S)+\frac{\partial}{\partial x_i}\left(D_{ij}\frac{\partial S}{\partial x_j}\right)+\frac{q_s}{\theta}S^*-R^{bio}_{sink,s}=R_s\frac{\partial S}{\partial t}, \tag{1}$$

where S is the aqueous phase substrate concentration [$M_{ls}\,l^{-3}$]; S^* is the hydrocarbon point source concentration [$M_{ls}\,l^{-3}$]; v_i is the average pore water velocity [$l\,T^{-1}$]; x_i is distance [L]; D_{ij} is the tensor for the hydrodynamic dispersion coefficient [$L^2\,T^{-1}$]; $R^{bio}_{sink,s}$ is a biodegradation sink term dependent on the mode of respiration [$M_{ls}\,l^{-3}\,T^{-1}$]; R_s is the retardation factor [–]; and t is time [T]; θ is aquifer porosity [–]; and q_s is the volumetric flux of water per unit volume of aquifer [T^{-1}] with $q_s > 0$ for sources and $q_s < 0$ for sinks.

Mass balance of the aqueous phase EAs (oxygen and sulfate) is

$$-\frac{\partial}{\partial x_i}(v_i E_{le})+\frac{\partial}{\partial x_i}\left(D_{ij}\frac{\partial E_{le}}{\partial x_j}\right)+\frac{q_s}{\theta}E^*_{le}-R^{bio}_{sink,le}=\frac{\partial E_{le}}{\partial t}, \tag{2}$$

where E_{le} is the aqueous phase concentration [$M_{le}\,l^{-3}$] of electron acceptor le (le = 1 for oxygen and le = 3 for sulfate); E^*_{le} is the EA point source concentration [$M_{le}\,l^{-3}$]; and $R^{bio}_{sink,le}$ is the EA biodegradation sink term [$M_{le}\,l^{-3}\,T^{-1}$].

Bioavailable Fe(III), associated with the solid phase, is subject to utilization only, and the expression of mass balance is

$$-R^{Bio}_{sink,le}=\frac{dE_{le}}{dt}, \tag{3}$$

where le = 2 for Fe(III); and E_{le} is the solid phase EA concentration [$M_{le}\,M^{-1}_{solid}$].

The equation of mass balance for TEAP end products (Fe(II) and methane) is

$$-\frac{\partial}{\partial x_i}(v_i P_{lp})+\frac{\partial}{\partial x_i}\left(D_{ij}\frac{\partial P_{lp}}{\partial x_j}\right)+\frac{q_s}{\theta}P^*_{lp}+R^{bio}_{source,lp}=R_{lp}\frac{\partial P_{lp}}{\partial t}, \tag{4}$$

where P_{lp} is the aqueous phase end product concentration [$M_{lp}\,l^{-3}$] (lp = 1 for Fe(II) and lp = 2 for methane); P^*_{lp} is the product point source concentration [$M_{lp}\,l^{-3}$]; $R^{bio}_{source,lp}$ is a biodegradation source term dependent on the mode of biogeneration [$M_{lp}\,l^{-3}\,T^{-1}$]; and R_{lp} is the end product retardation factor [–].

The respective mass balance expressions for the chlorinated ethenes (lc = 1, 2, and 3) and reductive dechlorination end products (ethene and chloride, lc = 4 and 5, respectively) are

$$-\frac{\partial}{\partial x_i}(v_i C_{lc})+\frac{\partial}{\partial x_i}\left(D_{ij}\frac{\partial C_{lc}}{\partial x_j}\right)+\frac{q_s}{\theta}C^*_{lc}+\Sigma R_{source/sink,lc}=R_{lc}\frac{\partial C_{lc}}{\partial t}, \tag{5a}$$

$$-\frac{\partial}{\partial x_i}(v_i C_{lc})+\frac{\partial}{\partial x_i}\left(D_{ij}\frac{\partial C_{lc}}{\partial x_j}\right)+\frac{q_s}{\theta}C^*_{lc}+R^{bio}_{source,lc}=R_{lc}\frac{\partial C_{lc}}{\partial t}, \tag{5b}$$

where C_{lc} is the chlorinated ethene/reductive dechlorination end product concentration [$M_{lc}\,l^{-3}$]; C^*_{lc} is the point source concentration [$M_{lc}\,l^{-3}$]; R_{lc} is the retardation factor [–]; and $\Sigma R_{source/sink,lc}$ is the sum of all sources and sinks:

$$\sum R_{source/sink,lc}=-R^{bio,EA}_{sink,lc}+R^{bio}_{Source,lc}+R^{DNAPL}_{source,lc} \tag{6}$$

where $R^{bio,EA}_{sink,lc}$ is a biodegradation sink term to account for the reduction of a chlorinated ethene [$M_{lc}\,l^{-3}\,T^{-1}$]; $R^{bio}_{source,lc}$ is a biodegradation source term to account for the production of *cis*DCE, VC, ethene, and chloride [$M_{lc}\,l^{-3}\,T^{-1}$]; and $R^{DNAPL}_{source,lc}$ is a source term for the dissolution of TCE from a NAPL source [$M_{lc}\,l^{-3}\,T^{-1}$];

Biodegradation kinetics

Mass loss of the organic carbon substrate due to biodegradation is expressed as the sum of aerobic and anaerobic processes, which are a function of organic carbon substrate and electron acceptor concentrations. The overall rate of hydrocarbon utilization is calculated using

$$R^{Bio}_{sink,s}=\sum_x\frac{M_x}{\theta}\left(\sum_{le}v^{max}_{x,s,le}\left[\frac{\overline{S}}{\overline{K}^s_{x,ls,le}+\overline{S}}\right]\left[\frac{\overline{E}_{le}}{\overline{K}^e_{x,le}+\overline{K}_{le}}\right]I_{le,li}\right), \tag{7}$$

where M_x is the mass of microbial population x per bulk volume of aquifer [$M\,l^{-3}$]; $v^{max}_{x,s,le}$ is the maxi-

mum specific utilization rate for a microbial population x growing on the substrate and using electron acceptor le [M M^{-1} T^{-1}]; $\overline{S}$ is the effective substrate concentration [M l^{-3}] (defined as the difference between the aqueous phase concentration and the minimum concentration below which biodegradation ceases); and $\overline{E}_{le}$ is the effective concentration of electron acceptor le [M l^{-3}]. $\overline{K}^{s}_{x,s,le}$ is the effective substrate half-saturation constant for utilization of an electron acceptor le [M l^{-3}]; $\overline{K}^{e}_{x,le}$ is the effective half-saturation constant for electron acceptor le [M l^{-3}]; $I_{le,li}$ is an inhibition function defined by

$$I_{le,li} = 1 \quad \text{for le} = 1 \tag{8a}$$

and

$$I_{le,li} = \prod_{li=1}^{le-1}\left[\frac{\kappa_{le,li}}{\kappa_{le,li} + \overline{E}_{li}}\right] \quad \text{for le} = 2, 3 \text{ or } 4, \tag{8b}$$

where $\kappa_{le,li}$ is the electron acceptor inhibition coefficient [M l^{-3}] representing inhibited utilization of electron acceptor le in the presence of electron acceptor li. Under methanogenic conditions, the electron acceptor Monod term in Equation (7) is not present.

Similarly, consumption of aqueous-phase EAs during biodegradation is

$$R^{Bio}_{sink,le} = \frac{M_x}{\theta}\gamma_{x,s,le} v^{max}_{x,s,le}\left[\frac{\overline{S}}{\overline{K}_{x,s,le} + \overline{s}}\right]\left[\frac{\overline{E}_{le}}{\overline{K}^{e}_{x,le} + \overline{E}_{le}}\right] I_{le,li}, \tag{9}$$

where $\gamma_{x,s,le}$ is the electron acceptor use coefficient [M M^{-1}], representing the mass of electron acceptor le used per unit mass of substrate. Fe(III) utilization (x = le = 2) is a zero-order expression with respect to Fe(III):

$$R^{Bio}_{sink,le} = \frac{M_x}{\rho_b}\gamma_{x,s,le} v^{max}_{x,s,le}\left[\frac{\overline{S}}{\overline{K}_{x,s,le} + \overline{s}}\right] I_{le,li}, \tag{10}$$

where ρ_b is the bulk density of the aquifer matrix [M$_{solid}$ l^{-3}]. Equation (10) is zero in the event that microbial utilization results in depletion of Fe(III).

The Fe(II) and methane source terms (lp = 1 and 2, respectively) are functions of the rate of Fe(III) (x = le = 3) and substrate utilization, respectively

$$R^{Bio}_{source,lp} = \zeta_{x,le} R^{Bio}_{sink,le}, \tag{11a}$$

$$R^{Bio}_{source,lp} = \zeta_{x,s} R^{Bio}_{sink,s}, \tag{11b}$$

where $\zeta_{x,le}$ and $\zeta_{x,s}$ are the Fe(III) and methane product generation coefficients [M M^{-1}].

The sink term for the reductive dechlorination process is expressed

$$R^{bio,EA}_{sink,lc} = \frac{M_y}{\theta} v^{max,EA}_{lc}\left[\frac{\overline{C}_{lc}}{\overline{K}^{e}_{lc} + \overline{C}_{lc}}\right] I_{lc,li}, \tag{12}$$

where M_y is the microbial biomass concentration of chlorinated ethene reducers [M$_b$ l$^{-3}_{pm}$]; $v^{max,EA}_{lc}$ is the maximum rate of reductive dechlorination for a chlorinated ethene lc [M$_{lc}$ M$_b^{-3}$T^{-1}]; K^{e}_{lc} is the effective half saturation constant for a chlorinated ethene (serving as an EA) lc [M$_{lc}$ l^{-3}]; $\overline{C}_{lc}$ is the effective concentration of a chlorinated ethene lc [M$_{lc}$ l^{-3}]; and $I_{lc,li}$ is an inhibition function defined by

$$I_{lc,li} = \prod_{li=1}^{3}\left[\frac{\kappa_{lc,li}}{\kappa_{lc,li} + \overline{E}_{li}}\right] I_{lc,lj}, \tag{13a}$$

where

$$I_{lc,lj} = 1 \quad \text{for lc} = 1 \text{ (TCE)} \tag{13b}$$

and

$$I_{lc,lj} = \prod_{lj=1}^{lc-1}\left[\frac{\kappa_{lc,lj}}{\kappa_{lc,lj} + \overline{C}_{lj}}\right] \quad \text{for lc} = 2 \text{ or } 3, \tag{13c}$$

where $\kappa_{lc,li}$ is the EA inhibition coefficient [M$_{le}$ l^{-3}] representing inhibition of the use of a chlorinated ethene lc (as an EA) by EA li (where li = 1, 2 or 3); $\kappa_{lc,lj}$ is the EA inhibition coefficient [M$_{le}$ l^{-3}] representing inhibition of the use of a chlorinated ethene lc (as an EA) by a higher molecular weight chlorinated ethene lj. It is assumed that the microbial population, M_y, only gain energy by respiring chlorinated ethenes and do not directly contribute to other TEAPs.

Production of a chlorinated daughter product and end products of reductive dechlorination (ethane and chloride) is expressed in terms of the rate of reduction of the parent compound

$$R^{bio}_{source,lc} = \zeta^{dau}_{lc,lc-1} R^{bio,EA}_{sink,lc-1}, \tag{14}$$

where $\zeta^{dau}_{lc,lc-1}$, is the daughter product generation coefficient [M$_{lc}$ M$^{-1}_{lc-1}$].

NAPL dissolution

For each chlorinated ethenes lc, the driving force for dissolution is the difference between the aqueous phase concentration (C_{lc}) and the equilibrium concentration (C_{lc}^{eq}), calculated using Raoult's Law as the product of the solubility of pure chlorinated ethene lc in water (C_{lc}^{sol}) and the mole fraction (f_{lc}) in the NAPL phase

$$f_{lc} = \frac{C_{lc}^{NAPL}/\omega_{lc}}{I^{NAPL}/\omega_{I} + \sum_{ls=1}^{NS} C_{lc}^{NAPL}/\omega_{lc}}, \tag{15}$$

where C_{lc}^{NAPL} is the NAPL mass of chlorinated ethene lc per unit mass dry soil [$M_{lc}\,M_{solid}^{-1}$]; I^{NAPL} is the NAPL concentration of inert constituents [$M_{I}\,M_{solid}^{-1}$]; and ω_j is the molecular weight of NAPL constituent j.

The rate of NAPL release, $R_{source,lc}^{NAPL}$, is a function of the phase concentration differential

$$R_{source,lc}^{NAPL} = \max\lfloor 0, k^{NAPL}(C_{lc}^{eq} - C_{lc})\rfloor, \tag{16}$$

where k^{NAPL} is the mass transfer rate coefficient [T^{-1}]. With each time step, C_{lc}^{NAPL} is updated by solving an equation of the mass balance of each NAPL-phase constituent

$$\frac{dC_{lc}^{NAPL}}{dt} = -\frac{\theta}{\rho_b} R_{source,lc}^{NAPL}. \tag{17}$$

Microbial growth kinetics

The mass balance equations for the growth and death of microbial populations x and y, respectively, are

$$\frac{1}{M_x}\frac{dM_x}{dt} = -k_{d_x} + Y_{x,s,le} v_{x,s,le}, \tag{18a}$$

$$\frac{1}{M_y}\frac{dM_y}{dt} = -k_{d_y} + Y_{y,lc} v_{y,lc}, \tag{18b}$$

where k_{d_x} and k_{d_y} are the microbial death rates [T^{-1}] and $Y_{x,s,le}$ and $Y_{y,lc}$ are the biomass yield coefficients [$M\,M^{-1}$] for the microbial populations x and y, respectively; $v_{x,s,le}$ is the specific rates of substrate utilization for microcolony x utilizing EA le [$M_{ls}\,M_b^{-1}\,T^{-1}$]; and $v_{x,lc}$ is the specific rates of utilization for microcolony y utilizing chloroethene lc [$M_{lc}\,M_b^{-1}\,T^{-1}$].

Model application

To illustrate the mathematical model and predictive simulation capabilities, two models are presented: a generic model and an interpretive (site) model. The objective of the generic model is to demonstrate (1) the simulation of TCE transport and reductive dechlorination in aquifers with differing redox conditions under a MNA scenario and (2) the simulation the temporal changes in the redox conditions and subsequent attenuation of TCE plume following the passive introduction of a dissolved substrate to an aerobic ground-water system (i.e., accelerated NA). The objective of the second model is to assess the ability of SEAM3D to simulate the transient response observed at a TCE-contaminated field site where a dissolved organic carbon substrates (fructose and lactate) were injected to accelerate natural attenuation (specifically, reductive dechlorination).

Generic models for monitored and accelerated natural attenuation

The model domain and generalized boundary conditions for the generic solute transport model are illustrated in Figure 1. The finite difference model grid consists of a single model layer model with 60 rows and 200 columns. Models cells are uniform (3.0 m) in both horizontal directions and vertical thickness (6.5 m). The MODFLOW layer type is designated to simulate an unconfined aquifer under steady-state flow conditions. A uniform ground-water flow field is simulated by imposing specified-head conditions on the influent and effluent boundaries ($h = 6.0$ and 5.0 m, respectively) of the domain at $x = 0$ and 200 m, respectively. By assuming a homogeneous aquifer with a hydraulic conductivity and porosity of $10.2\,m\,d^{-1}$ and 0.30, respectively, and no-flow boundary conditions at $y = 0$ and 60 m, the result is a uniform, unidirectional velocity of $0.057\,m\,d^{-1}$.

Initial concentrations for the chlorinated ethenes (TCE, *cis*DCE, and VC), organic carbon, and reaction endproduct (Fe(II), methane, chloride, and ethene) are zero. The 8-cell wide by 4-cell long NAPL source is designed to simulate a highly-concentrated TCE spill of approximately $100\,m^3$, resulting in a constant source concentration ($750\,mg\,l^{-1}$) over the entire simulation period of

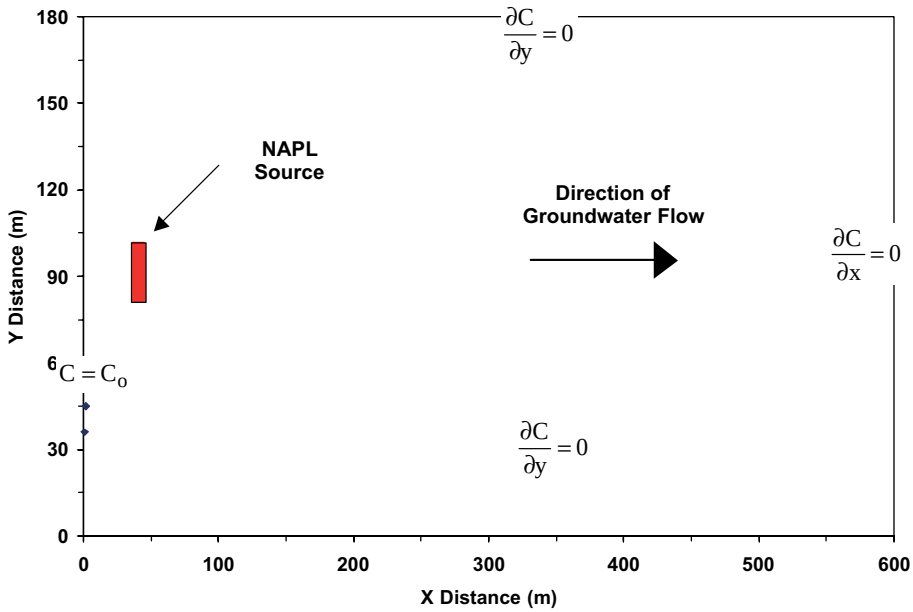

Figure 1. Model domain and generalized boundary conditions for the generic model simulations of TCE transport under conditions representing monitored natural attenuation and accelerated natural attenuation (dissolved carbon addition).

20 year. Background EA concentrations (oxygen, Fe(III), and sulfate), shown in Table 1, reflect the dominant TEAP associated with each of the three model scenarios: aerobic, iron-reducing, and strongly-reducing ground-water system. Table 2 includes maximum specific rates of reductive dechlorination, half-saturation constants, and inhibition coefficients for each of the chlorinated ethenes based on a previous study (Widdowson et al. 2001). Effective rates of reductive dechlorination (Table 3) are calculated using Equation (19) based on the background EA concentrations, and maximum simulated chlorinated ethene concentrations and the parameters listed in Table 2:

$$v_{lc}^{EA} = v_{lc}^{max,EA}\left[\frac{\overline{C}_{lc}}{\overline{K}_{lc}^{e} + \overline{C}_{lc}}\right] I_{lc,li}, \qquad (19)$$

Table 1. Initial concentration of electron acceptors (EAs) for the three generic models

TEAP	Initial EA Concentration[a]		
	O_2	Fe(III)	SO_4^{2-}
Aerobic	4.0	30	15
Fe(III)-reducing	0	30	15
Sulfate-reducing/methanogenic	0	0	15

[a]Units = mg/l for O_2 and SO_4^{2-}; mg/g for Fe(III).

Table 2. Maximum specific rates of reductive dechlorination ($v_{lc}^{max,EA}$), half-saturation constants ($\overline{K}_{lc}^{e}$), and inhibition coefficients for each of the chlorinated ethenes simulated in the generic models

Chlorinated ethene	$v_{lc}^{max,EA}$ (d^{-1})	$\overline{K}_{lc}^{e}$ (g m^{-3})	Inhibition coefficient[a]				
			O_2	Fe(III)	SO_4^{2-}	TCE	*cis*DCE
TCE	0.20	12.0	0.01	25	18	N/A	N/A
*cis*DCE	0.16	7.0	0.01	5	18	50	N/A
VC	0.14	0.35	0.01	5	18	0.01	0.15

[a]Units = mg/l for O_2 and SO_4^{2-}; mg/g for Fe(III).

Table 3. Effective rates of reductive dechlorination for the simulated chlorinated ethenes based on the initial condition of the EAs (Table 1), TCE source concentration (700 mg/l), reductive dechlorination rate parameters (Table 2) for the generic models

TEAP	Effective reductive dechlorination rate (mg/l day^{-1})					
	TCE	*cis*DCE		VC		
		TCE present	TCE absent	TCE present	TCE[(a)] absent	*cis*DCE absent
Aerobic	1.3×10^{-5}	1.4×10^{-10}	1.0×10^{-5}	1.2×10^{-10}	8.2×10^{-7}	1.7×10^{-5}
Fe(III)-reducing	0.036	5.3×10^{-4}	7.9×10^{-3}	1.3×10^{-8}	9.1×10^{-4}	6.9×10^{-3}
Sulfate-reducing/ methanogenic	0.11	0.0058	0.087	$1.4x10^{-7}$	0.010	0.076

[(a)]Based on a *cis*DCE concentration of 1.0 mg/l.

where the effective rate of reductive dechlorination is the product of the maximum rate, Monod term, and the inhibition function.

Site model for accelerated natural attenuation

A site model is developed to simulate a recirculated dissolved-phase substrate for accelerated natural attenuation at the Naval Support Activity Mid South located in Millington, Tennessee. TCE sources are present under a concrete aircraft apron at depths up to 75 feet below land surface in fluvial deposits consisting of poorly sorted sand, gravel and minor amounts of interstitial clay material (Casey et al. 2002). Local hydraulic gradient is approximately $0.006\,m\,m^{-1}$ and an estimated groundwater velocity of 9.4–19 m $year^{-1}$. Over approximately 260 days, water was extracted from a single well at an average flow rate of $15\,l\,min^{-1}$. Substrate delivery consisted of continuous injection of dissolved carbon sources (fructose for the first 60 days of the test, followed by sodium lactate) at two wells located 35 m upgradient of a single pumping well (Casey et al. 2002). Substrate addition was intended to create a reducing condition *via* the consumption of electron acceptors and promote reductive dechlorination of TCE.

The groundwater flow model is constructed using the MODFLOW code using a two-step process. The objective of the first flow model is to simulate the flow field during the pilot test and determine the boundary conditions of a fine-mesh model grid. The objective of the finemesh flow model (nested inside the first model grid) is to simulate the local flow field in the vicinity of the injection and pumping wells for the transport simulation. The larger model domain consists of 41 rows, 74 columns, and 3 layers (7.5-m by 7.5-m by 5.0-m cells, respectively) with specified flow boundaries located upgradient and downgradient of the pilot test and with no-flow boundaries parallel to the natural gradient. The flow model is calibrated to the field-measured horizontal hydraulic gradient and pumping rates.

After determining that vertical flow has minimal impact on the overall flow field, the fine-mesh

Table 4. Biodegradation parameters for simulation of accelerated natural attenuation (generic and site models)

Microbial population	$\nu^{max}_{x,s,le}$ (d^{-1})	$\overline{K}^{s}_{x,s,le}$ (g m^{-3})	$\overline{K}^{e}_{x,le}$ (g m^{-3})	$Y_{x,ls,le}$ (g g^{-1})	$\gamma_{x,s,le}$ (g g^{-1})	ζ_x (g g^{-1})	$\kappa_{le,li}$ (g m^{-3})		
							O_2	Fe(III)	SO_4^{2-}
Aerobes	0.50	5.0	1.0	0.25	3.0	N/A	N/A	N/A	N/A
Iron reducers	0.025	10.0	N/A	0.20	25.0	0.10	0.20	N/A	N/A
Sulfate reducers	0.010	15.0	10.0	0.15	4.0	N/A	0.10	30.0	N/A
Methanogens	0.005	20.0	N/A	0.10	N/A	0.20	0.05	15.0	5.0

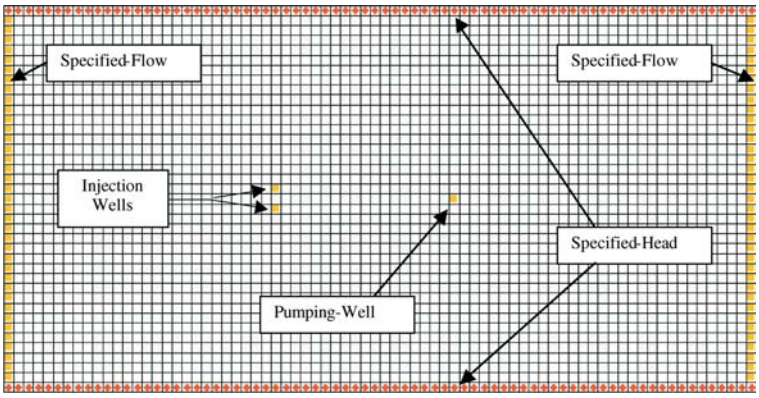

Figure 2. Model domain, generalized boundary conditions, and pumping/injection well locations for a fine-mesh solute transport model developed to simulate a recirculating accelerated natural attenuation pilot test at a TCE-contaminated site.

flow and transport model grid (Figure 2) consists of a single model layer model with 39 rows and 76 columns. Models cells are uniform (2.5 m) in both horizontal directions and vertical thickness (5.0 m). Boundary conditions include specified flow upgradient and downgradient of the injection and pumping wells and specified head along the lateral boundaries (both determined from the results of the first flow model).

Three stress periods are used in the local flow and transport model simulation: (1) a 90-day period during which the equilibrium TCE source concentration reaches the field-measured value (2.1 mg/l), (2) the 270-day pilot test, and (3) a 360-day post-test period. The initial conditions for the electron acceptors at the start of Stress Period 1 (oxygen = 2.5 mg/l and sulfate = 8.0 mg/l) are based on the pre-treatment concentrations. The starting level of Fe(III), a calibration parameter, is 200 mg/kg. Initial conditions of all other transport model constituents are zero.

Results and discussion

Simulation of monitored natural attenuation

Figure 3 depicts the simulated concentration distribution of TCE at 20 years in three different ground-water systems: aerobic (3a), iron-reducing (3b), and strongly-reducing (3c) conditions. The TCE plume in the aerobic ground-water system is approximately twice as large and wide as the TCE plume simulated under strongly-reducing conditions. In these simulations, the sole attenuation process is reductive dechlorination, and the degree of attenuation (and thus, the dimensions of and concentrations in the TCE plume) is controlled by the predominant TEAP. However, because natural organic carbon is sustaining the TEAPs over the simulation period, there is no temporal or spatial variability demonstrated in the three examples.

Figure 4 shows plots of concentration profiles of TCE, *cis*DCE, and VC along the centerline of the plume for each of the three ground-water systems: aerobic (top), iron-reducing (middle), and strongly-reducing (bottom). The trends in the TCE concentration distribution noted above are depicted in the three plots. Consistent with the notion that reductive dechlorination is not a significant attenuation mechanism for TCE in aerobic systems, Figure 4 (top) shows the absence of chlorinated progeny and relatively high concentrations of TCE along the length of the plume. In the iron-reducing system (Figure 4 middle), the attenuation of the TCE plume (relative to the aerobic system) and the formation of *cis*DCE suggests a moderate degree of reductive dechlorination occurs, but both *cis*DCE and VC are transported beyond the toe of the TCE plume at distances (~540 m) comparable to the aerobic system. Direct anaerobic oxidation was not incorporated in the simulation results. In contrast, all of the chlorinated ethenes in the strongly-reducing system (Figure 4 bottom) are attenuated, and the toe of the VC plume is located at 360 m.

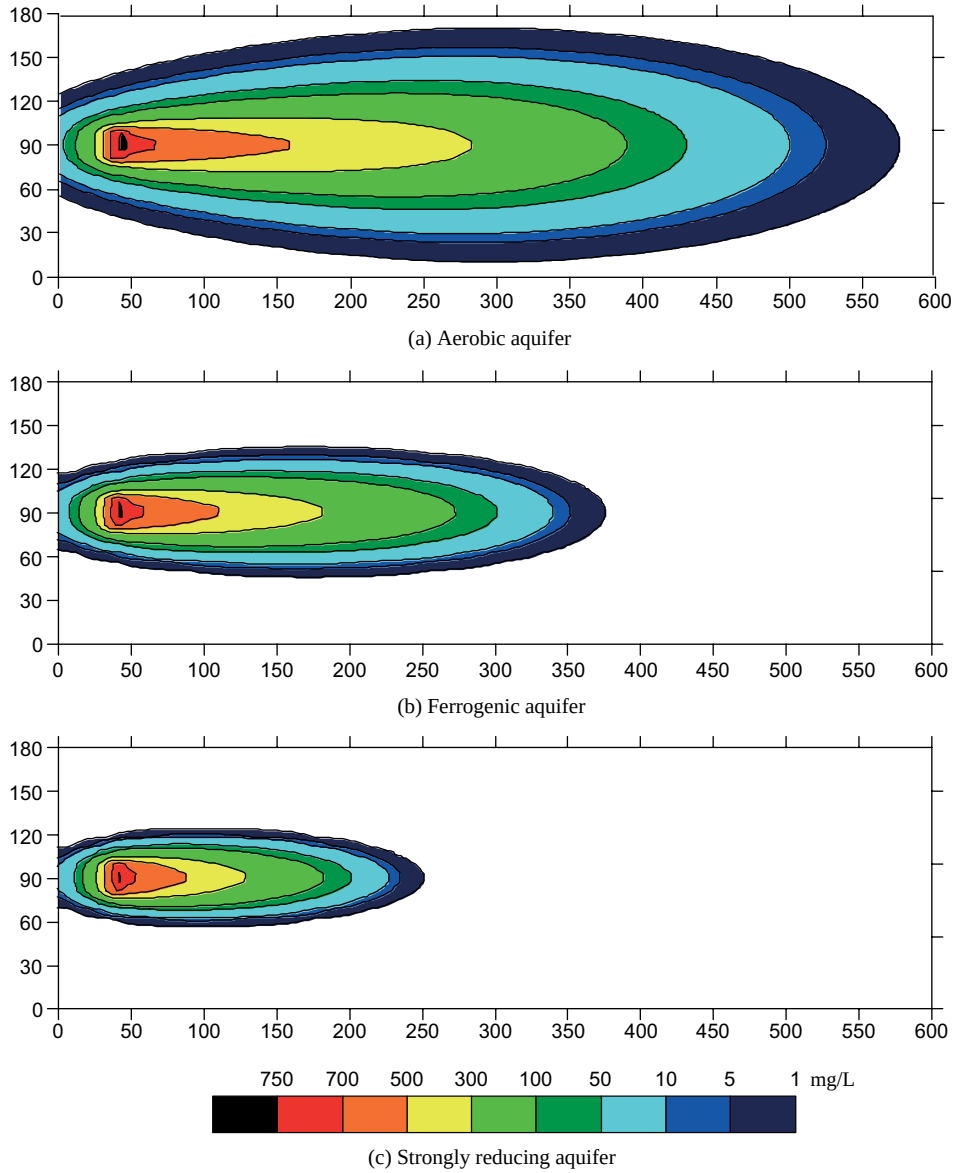

Figure 3. Simulated TCE plumes at 20 years emanating from a NAPL source for three groundwater systems: aerobic (top), iron-reducing (middle), and strongly-reducing (bottom).

Simulation of passive system for accelerated natural attenuation

The previous results demonstrate the numerical capabilities of the model for simulating the spatial distribution of chlorinated ethenes and the dependence of reductive dechlorination on the ambient TEAP. For the simulation of the accelerated NA problem, specified-concentration cells were added to the MNA model grid at a location immediately upgradient of the NAPL source to simulate an organic carbon substrate introduced using a 6-m long by 36-m wide trench. Figure 5 (top) shows the initial condition of TCE in the aerobic ground-water system ten years after the NAPL source begins to pollute the aquifer. Without the introduction of a reducing agent and with no other ERA, the plume continues to

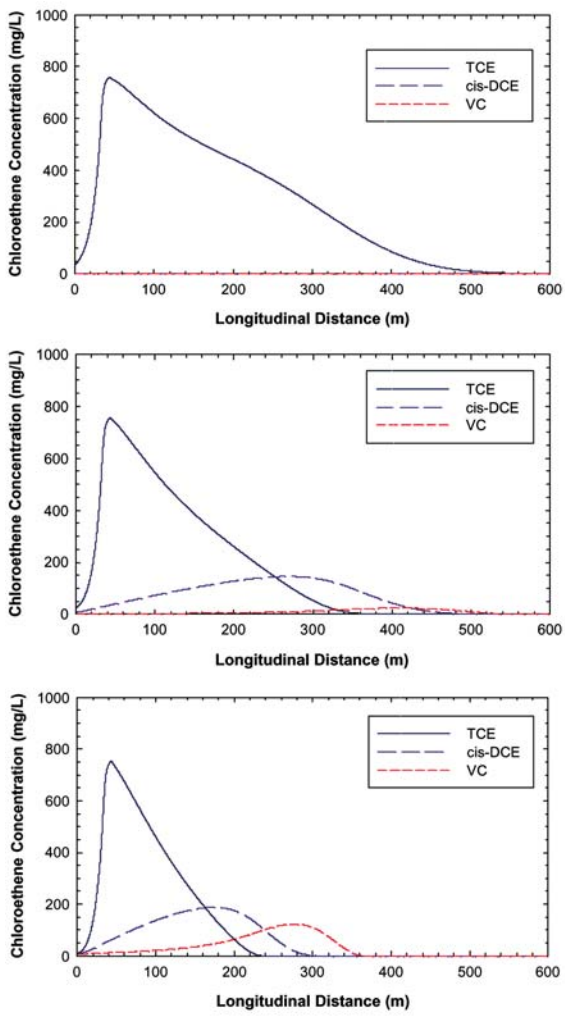

Figure 4. Concentration profiles of TCE, *cis*DCE, and VC along the plume centerline at 20 years for three ground-water systems: aerobic (top), iron-reducing (middle), and strongly-reducing (bottom).

expand over the next 10 years (Figure 5, middle), which is identical to the TCE plume depicted in Figure 3 (top). In comparison, Figure 5 (bottom) shows the effect of the carbon source on the TCE plume over the same 10-year period as the dissolved substrate mixes with the NAPL source. At year 20 (10 years following continuous treatment) a smaller TCE plume is evolving in the vicinity of the source. However, further downgradient of the source (~150 m), the impact of the *in situ* bioremediation system is not observed as the TCE plume expands in width and length and a fragment of the initial plume is breaking off as evidence by the peak concentration at 250 m.

Figure 6 depicts the concentration distributions of the dissolved substrate (top), oxygen (middle), and sulfate (bottom) ten years following the introduction of the reducing agent to the aquifer. A wide-spread anaerobic zone is present in the vicinity of the NAPL source and over a 200-m footprint that coincides with the shrinking TCE plume and the transported organic carbon substrate. The continuous supply of substrate eliminates the dissolved oxygen (DO) and much of the sulfate present in the ambient ground water, which flows into the TCE source zone and plume. However, the footprint of sulfate consumption is smaller than the zone of depleted DO as the latter EA is preferentially utilized.

Figure 7 (top) illustrates the spatial relationship between the organic carbon substrate and DO along the centerline of the TCE plume at year 20, which is similar to that observed at petroleum hydrocarbon sites. Aerobic conditions dominate the system ahead of the substrate front, and the anaerobic TEAPs exhibit a distributed pattern behind the front. Figure 7 (middle) shows that in the anaerobic core of the TCE plume, Fe(III) is consumed over a distance from 30 to 200 m. In this same zone, sulfate enters with the ambient ground-water flow and is consumed, and methane is produced as the substrate is subjected to methanogenic-mediated biodegradation. The gradual rise in Fe(III) from 200 to 300 m and the presence of Fe(II) in the aqueous phase suggests that iron-reduction is active downgradient of the strongly reducing zone.

These results demonstrate the potential effectiveness and limitation of a passive system designed to enhance reductive dechlorination. In this example, the anaerobic zone in the vicinity of the source zone creates ideal conditions for *in situ* bioremediation of the chlorinated ethenes. However, the timeframe required for the substrate front to advance and the anaerobic zone to develop in a passive system is entirely dependent on the ambient ground-water velocity. Furthermore, the substrate source must be sustained during the period required to treat the NAPL source zone. In addition, this approach does little to attenuate that portion of the TCE plume downgradient of the source where a point of regulatory compliance may exist. In this case, another treatment or containment option would be necessary in combination with the passive system.

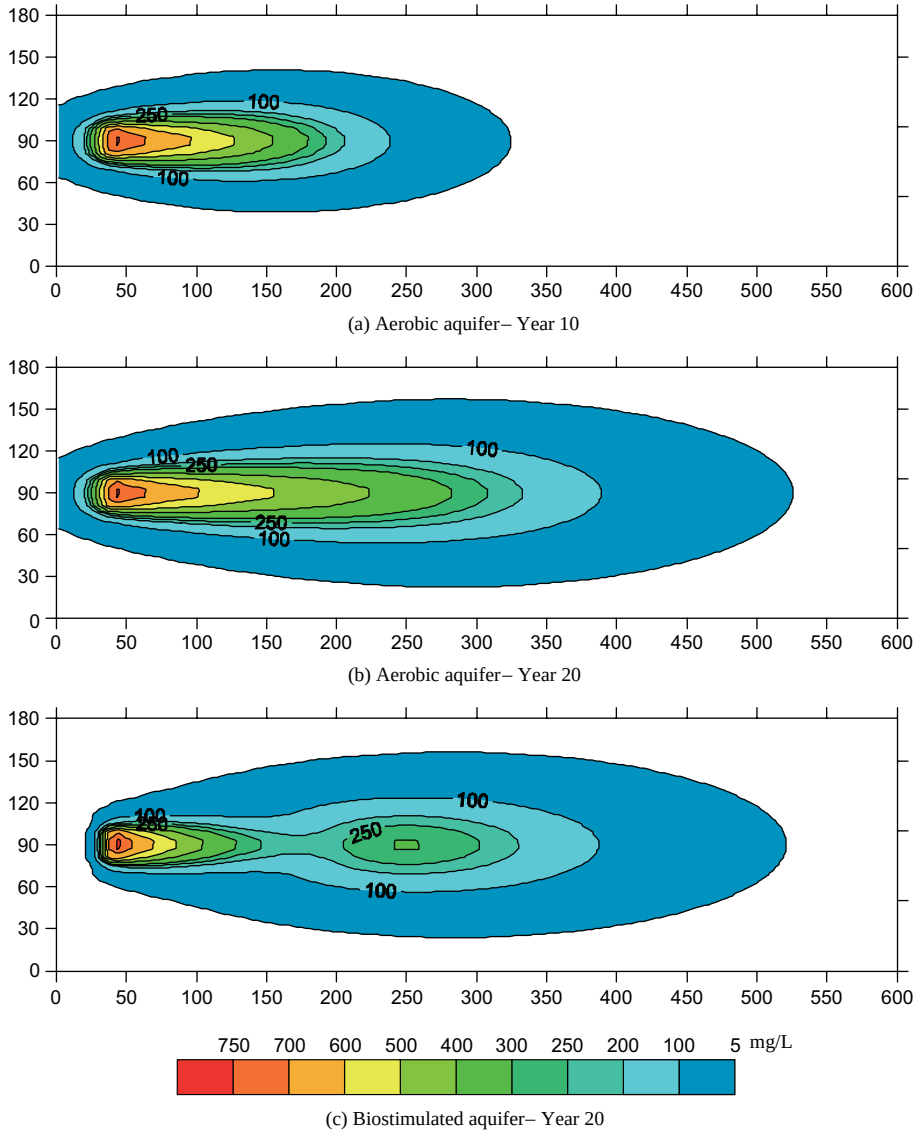

Figure 5. Simulated TCE plumes in an aerobic ground-water system at 10 years (top) and 20 years without and with the continuous addition of a reducing agent initiated at the end of year 10 (middle and bottom, respectively).

Site model of accelerated natural attenuation

The fine-mesh site solute model is calibrated by minimizing the error between the measured and simulated concentration of the chlorinated ethenes, beginning with TCE. Measured data are derived from a monitoring well located between the injection wells and the pumping wells where the pre-test levels of TCE were highest. Calibration of the solute transport model is accomplished through a trial-and-error approach. For calibration of the TCE data, the key parameters are the initial concentration of Fe(III), maximum rate of reductive dechlorination of TCE, and the initial biomass. Increasing the background concentration of Fe(III) results in an increasingly longer lag period before the TCE concentration began to decrease. Increases in $v_{lc}^{max,EA}$ and M_y result in greater decreases in the concentration of TCE following the lag period.

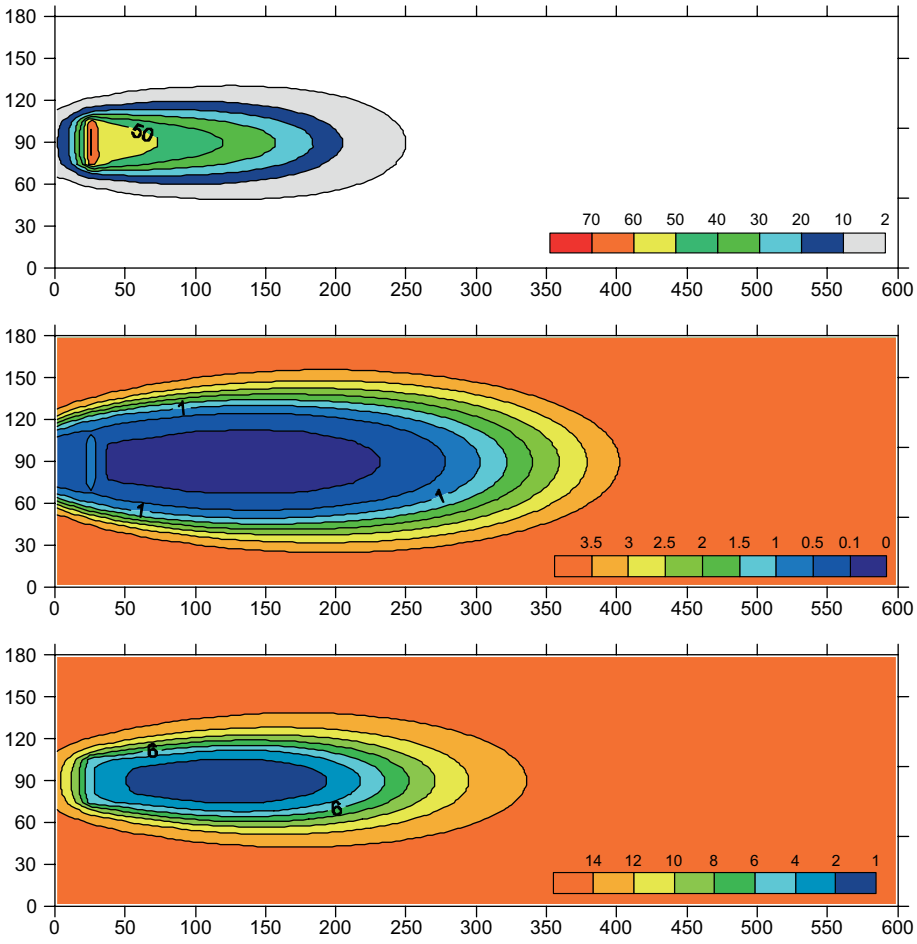

Figure 6. Concentration distributions of an organic carbon substrate (top), dissolved oxygen (middle), and sulfate (bottom) ten years following continuous addition of the substrate at a location immediately upgradient of a TCE source. Concentration units are mg/l for all solutes.

The model is next calibrated to the *cis*DCE and VC data, in successive order, after calibration to the TCE data. Calibration of the model to the *cis*DCE and VC data primarily involves adjustment of maximum rates of reductive dechlorination and the inhibition coefficients (TCE-*cis*DCE and *cis*DCE-VC). Decreases in the magnitude of $v_{lc}^{max,EA}$ result in higher peak values of *cis*DCE and VC following the drop in the concentrations of TCE and *cis*DCE, respectively. Increases in the *cis*DCE-VC inhibition coefficient well above the calibrated value result in a trend toward instantaneous production and consumption of VC. Because the injection of the substrate results in strongly reducing conditions within the zone of mixing, reductive dechlorination is the primary mechanisms for biotransformation of the chlorinated ethenes and the impact of direct oxidation on the concentration of *cis*DCE and VC is not significant.

Figure 8 shows time series for the simulated and measured chlorinated ethene data from Well 007G59LFA (located 17.5 m downgradient of the injection wells) beginning at the start of the second stress period (90 days). No substrate is injected prior to this phase of the experiment. At 90 days, the concentration of TCE is steady and the TEAP condition is aerobic. For approximately the next 90 days, only a small decrease in the TCE concentration along with a corresponding production of *cis*DCE are noted. As shown in Figure 9 (top), the model simulates a continual decrease in the EA

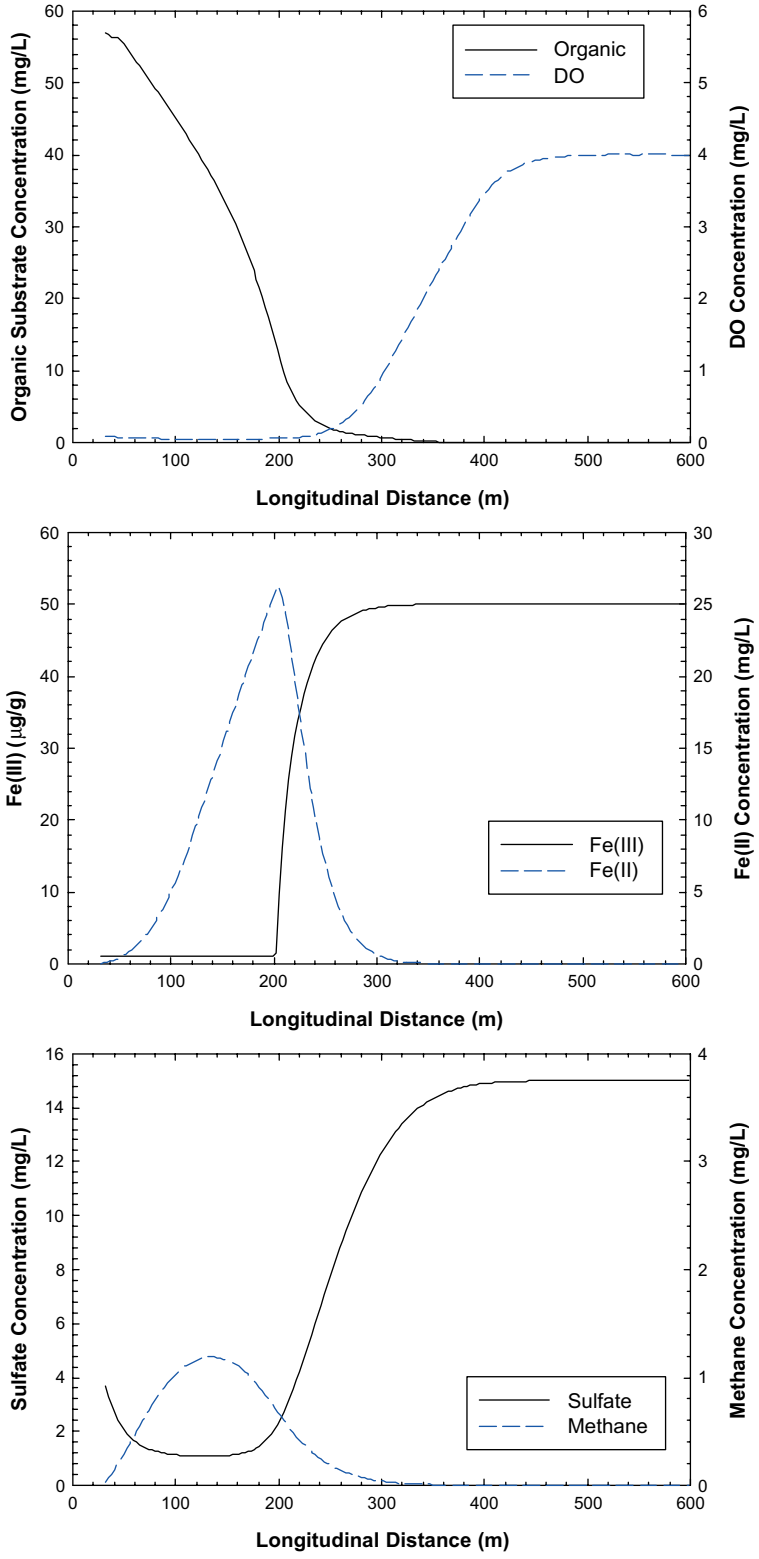

Figure 7. Concentration profiles of an organic carbon substrate and dissolved oxygen (top), Fe(III) and Fe(II) (middle), and sulfate and methane (bottom) along the TCE plume centerline at year 20, 10 years following continuous addition of the substrate at a location immediately upgradient of a TCE source.

concentrations during this same period as the front of injected substrate moves downgradient, followed by complete consumption of EAs around day 225. The production of methane and an end to the production of Fe(II) starting at day 225 (Figure 9, bottom) indicate that methanogenic conditions prevail in the vicinity of the monitoring well over the remaining test period. During this phase of the test (day 180 to day 280), a precipitous decline in TCE and production of *cis*DCE are observed (Figure 8). At day 280, a second equilibrium condition is reached where both TCE and *cis*DCE concentrations remain steady through the end of Stress Period 2 (day 360). Conditions for reductive dechlorination are optimal, but the travel time between the TCE source and the monitoring well is insufficient to observe VC production.

Beginning at day 360, the ground-water velocity decreases to pre-test levels at the start of Stress Period 3, and its effect is noted in Figure 8 with the decline in TCE concentration from 0.77 mg/l at day 360 to 0.050 mg/l at day 510. This results in conditions more favorable for reductive dechlorination of *cis*DCE and subsequent production of VC during the same period. The return to an ambient velocity results in a decrease in the travel time and an increase in attenuation. At day 510, a final equilibrium condition is reached where the concentrations of the chlorinated ethenes remain steady through the end of Stress Period 3 (day 720).

At the end of the pilot test (day 360), measurements of dissolved hydrogen in the treatment zone show that a mixture of methanogenic and sulfate-reducing conditions exist in the aquifer (Casey et al. 2002). These results are consistent with the model simulation, which also show that these conditions are maintained at least over the remainder of the simulated post-test period. Because this anaerobic zone of strongly reduced conditions are established not only downgradient of the injection wells and TCE source but also at locations upgradient (~25 m), the return of aqueous EAs in the ambient ground water (9.4–19 m/year) is not observed within the post-test monitoring period.

Conclusions

Consideration of the spatial distribution of and temporal changes in anaerobic TEAPs is essential to assessing the potential for reductive dechlorination and other microbially-mediated attenuation processes in ground-water systems contaminated with chlorinated ethenes (Chapelle 2001). Because the rate and extent of reductive dechlorination is

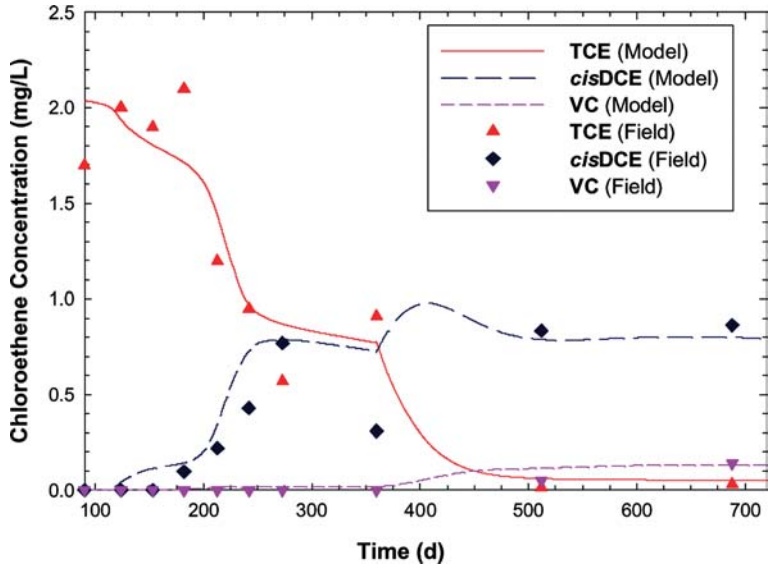

Figure 8. Field-measured and model-simulated TCE, *cis*DCE, and VC concentrations at a monitoring well during and following an accelerated natural attenuation pilot test at the Naval Support Activity Mid South.

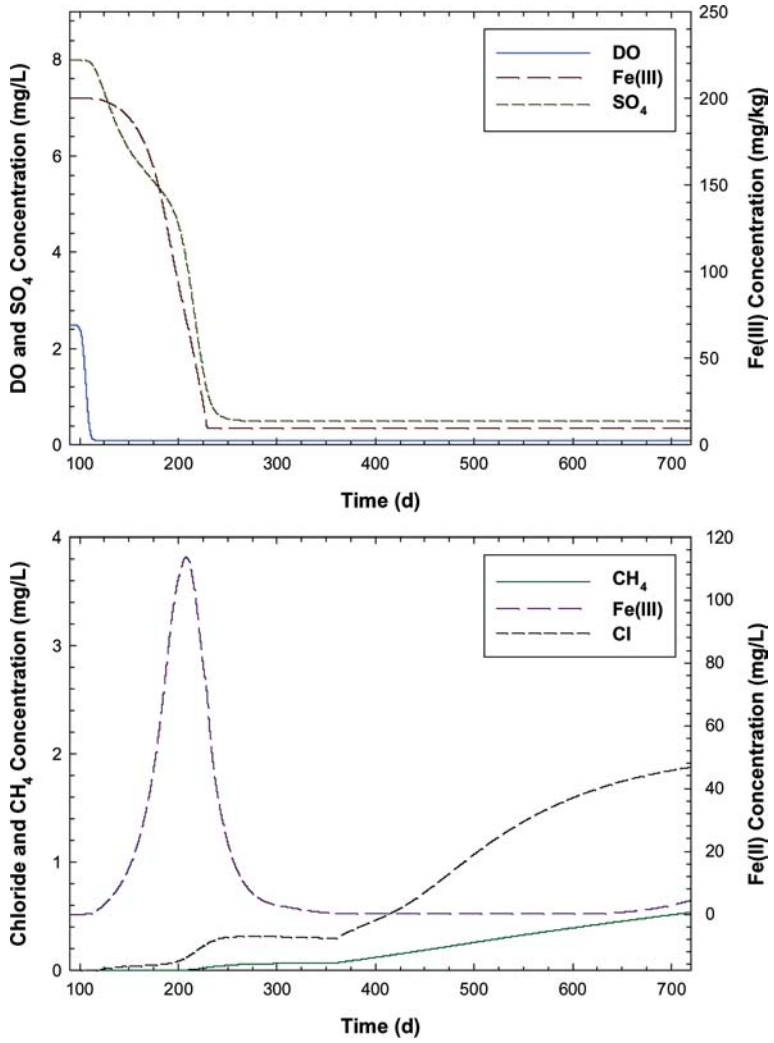

Figure 9. Simulated concentration versus time data for electron acceptors – dissolved oxygen, Fe(III), and sulfate (top) – and biodegradation end products – methane, Fe(II), and chloride (bottom) – during and following the *in-situ* bioremediation pilot test.

dependent on the redox condition (Bradley 2000), methods to incorporate anaerobic TEAPs in comprehensive numerical models are warranted. One approach to this problem is demonstrated in this study in which anaerobic TEAPs are simulated over space and time in the model grid. Simulation results of a 270-day pilot test to enhance *in situ* bioremediation of TCE and the 360-day post-test period demonstrate that the SEAM3D code provides an adequate means to predict the transient coupled behavior of chlorinated ethene biotransformation and redox conditions.

The utility of this approach is demonstrable in situations where reducing agents are added to create strongly reducing conditions and to enhance the *in situ* rate of reductive dechlorination. This approach is also applicable at 'Type 1' sites, where an anthropogenic source of organic carbon (e.g., petroleum hydrocarbon compounds) combined with TCE or PCE are present to drive reductive dechlorination (Wiedemeier et al. 1998). In cases where strongly reducing conditions can not be sustained due to depletion of the organic carbon source within the same timeframe as the chlorinated ethene source, then the ground-water system would be expected to revert to more oxic conditions over time, resulting in a decreased efficiency in the attenuation of the chlorinated ethenes. Be-

cause the simulated TEAP distribution is directly coupled to the availability of organic carbon, in theory, the modeling approach presented here could be used in a predictive mode to quantify the effects of source depletion on the transient response and spatial changes in the redox conditions in an aquifer and its impact on the attenuation of chlorinated ethenes.

Acknowledgements

Technical and financial support for this work was provided by the Southern Division Naval Facilities Engineering Command, Charleston, South Carolina. Primary funding for the development of SEAM3D work was received from the Strategic Environmental Research and Development Program (SERDP) of the U.S. Department of Defense, Environmental Protection Agency, and Department of Energy, as part of Project CU-1062, ''Development of Simulators for *In-Situ* Remediation Evaluation, Design, and Operation'', the U.S. Army Engineer Research and Development Center, Waterways Experiment Station (WES), lead agency.

References

Boulicault KJ, Hinchee RH, Wiedemeier TH, Hoxworth SW & Swingle TP (2000) Vegoil: a novel approach for stimulating reductive dechlorination. In: Wickramanayake GB, Gavaskar AR, Alleman BC & Magar VS (Eds) Bioremediation and Phytoremediation of Chlorinated and Recalcitrant Compounds (pp 62–64, 1–7). Battelle Press, Columbus, OH

Bradley PM & Chapelle FH (1996) Anaerobic mineralization of vinyl chloride in Fe(III)-reducing, aquifer sediments. Environ. Sci. Technol. 30: 2084–2086

Bradley PM (2000) Microbial degradation of chloroethenes in groundwater systems. Hydrogeol. J. 8: 104–111.

Casey CC, Britto R, Stedman J, Henry B, Weidemeier M & Reed J (2002) Field scale evaluation of soybean oil and dissolved substrates for *in situ* bioremediation. Third International Conference on Chlorinated and Recalcitrant Compounds, Monterey, CA, May 20–23, 2002

Chapelle FH (1996) Identifying redox conditions that favor the natural attenuation of chlorinated ethenes in contaminated ground-water systems. In: Symposium on Natural Attenuation of Chlorinated Organics in Ground Water, EPA/540/R-96/509 (pp. 17–20)

Chapelle FH (2001) Ground-Water Microbiology and Geochemistry, 2nd edn. J. Wiley & Sons, New York

Chapelle FH & Bradley PM (1998) Selecting remediation goals by assessing the natural attenuation capacity of groundwater systems. Bioremediation J. 2(3&4): 227–238

Charbeneau RJ (2000) Groundwater Hydraulics and Pollutant Transport, 1st edn. Prentice Hall, Upper Saddle River, NJ

Hansen MA, Burdick J, Lenzo FC & Suthersan S (2000) Enhanced reductive dechlorination: lessons learned at over twenty sites. In: Wickramanayake GB, Gavaskar AR, Alleman BC & Magar VS (Eds) Bioremediation and Phytoremediation of Chlorinated and Recalcitrant Compounds. C2–4 (pp 263–270). Battelle Press, Columbus, OH

Hartmans S, deBont JAM, Tramper J & Luyben KCAM (1985) Bacterial degradation of vinyl chloride. Biotechnol. Lett. 7: 383–388

Koenigsberg SS, Farone WA & Sandefur CA (2000) Time-released electron donor technology for accelerated biological reductive dechlorination. In: Wickramanayake GB, Gavaskar AR, Alleman BC & Magar VS (Eds.) Bioremediation and Phytoremediation of Chlorinated and Recalcitrant Compounds. C2–4 (pp 39–46). Battelle Press, Columbus, OH

National Research Council (2000) Natural Attenuation for Groundwater Remediation. National Academy Press, Washington, DC

U.S. Environmental Protection Agency (1999) Use of monitored natural attenuation at Superfund, RCRA corrective action, and underground storage tank sites. Final OSWER Monitored Natural Attenuation Policy (Oswer Directive 9200.4-17P). United States Environmental Protection Agency, Office of Solid Waste and Emergency Response

Vogel TM & McCarty PL (1985) Biotransformation of tetrachloroethylene to trichloroethylene, dichloroethylene, vinyl chloride, and carbon dioxide under methanogenic conditions. Appl. Environ. Microbiol. 49: 1080–1083

Waddill DW & Widdowson MA (1998) Three-dimensional model for subsurface transport and biodegradation. ASCE J. Environ. Eng. 124(4): 336–344

Waddill DW & Widdowson MA (2000) SEAM3D: A numerical model for threedimensional solute transport and sequential electron acceptor-based biodegradation in ground water. ERDC/EL TR-00-X, U.S. Army Engineer Research and Development Center, Vicksburg, MS

Waddill DW, Casey CC & Widdowson MA (2002) Modeling vegetable oil injection for enhanced biodegradation of chlorinated solvents. In: Gavaskar AR & Chen ASC (Eds) Remediation of Chlorinated and Recalcitrant Compounds

Widdowson MA, Rectanus HV, Novak JT & Berry DF (2001) Integrated assessment of monitored natural attenuation at a PCE contaminated site. In: Leeson A, Kelley ME, Rifai HS & Magar VS (Eds) Natural Attenuation of Environmental Contaminants. (pp 105–112) Battelle Press, Columbus, OH

Widdowson MA (2003) SEAM3D: a numerical model for three-dimensional solute transport and sequential electron acceptor-based biodegradation in ground water. Final Report to the U.S. Army Engineer Research and Development Center, Vicksburg, MS

Wiedemeier TH, Swanson MA, Moutoux DE, Gordon EK, Wilson JT, Wilson BH, Kampbell DH, Haas PE, Miller RN, Hansen JE & Chapelle FH (1998) Technical protocol for evaluating natural attenuation of chlorinated solvents in

ground water. US Environmental Protection Agency EPA/600/R-98-128

Wilson JT & Wilson BH (1985) Biotransformation of trichloroethylene in soil. Appl. Environ. Microbiol. 49: 242–243

Zheng C & Wang PP (1999) MT3DMS: a modular three-dimensional transport model for simulation of advection, dispersion, and chemical reactions of contaminants in ground water systems, SERDP-99-1, US Army Engineer Research and Development Center, Vicksburg, MS